Study of correlation states of acetylene by synchrotron photoelectron spectroscopy

Maria Sabaye Moghaddam, S. J. Dejardins, and A. D. O. Bawagan[a)]
Ottawa-Carleton Chemistry Institute, Carleton University, Ottawa, Ontario, K1S 5B6 Canada

K. H. Tan
Canadian Sychrotron Radiation Facility, University of Wisconsin, Stoughton, Wisconsin 53589

Y. Wang and E. R. Davidson
Department of Chemistry, Indiana University, Bloomington, Indiana 47405

(Received 19 May 1995; accepted 25 August 1995)

The inner valence photoelectron spectra of acetylene (C_2H_2) and isotopically labeled acetylene ($1,2^{13}C$–C_2H_2) are obtained using high resolution synchrotron photoelectron spectroscopy. Four distinct correlation (satellite) peaks, consistent with previous x-ray photoelectron spectroscopy measurements, are resolved. The photon energy dependence of the intensity ratios of these satellites to the $2\sigma_g^{-1}$ main peak is observed over a wide photon energy range (32–72 eV). Three of these satellites (26.6, 28.0, and 29.8 eV binding energy) exhibited constant photon energy dependence while the fourth satellite (31.2 eV binding energy) showed enhancement of intensity towards the threshold. The photon energy dependence of correlation (satellite) peak 4 can be explained in either of two ways: (1) Peak 4 is a dynamic correlation peak associated with the $2\sigma_g^{-1}$ ionization process or (2) peak 4 is an intrinsic correlation peak associated with the $3\sigma_g^{-1}$ ionization process. A multireference singles and doubles configuration interaction (MRSDCI-ANO) calculation of the theoretical photoelectron inner valence spectrum using average natural orbitals indicates that the latter explanation (2) is more likely. Semiquantitative agreement (in terms of the peak positions and intensities) is also obtained between the experimental photoelectron spectrum and the MRSDCI(ANO) calculation. © *1995 American Institute of Physics.*

I. INTRODUCTION

The experimental and theoretical study of electron correlation effects is central to a detailed understanding of the electronic structure of atoms and molecules.[1] Apart from the correlation energy (i.e., $E_{\text{exact}}-E_{\text{HF}}$), electron correlation effects are also manifested in the binding energy spectrum of atoms and molecules. A direct experimental method for obtaining binding energy spectra is photoelectron spectroscopy (PES) and for years the Hartree–Fock model has been successful in accounting for the main features of the photoelectron spectra especially in the outer-valence region. In general, a ''one ionization peak–one orbital'' correspondence can be established in the photoelectron spectrum; however, lower intensity, ''extra'' features are often times observed.[2,3] These features are called correlation peaks although they are also referred to as satellite peaks, shake-up peaks, or many-body peaks. [For consistency, the experimental phenomena will be referred to as ''correlation (satellite) peaks,'' and the theoretical representation or interpretation of these phenomena as ''correlation states'' or equivalently as excited states of the ion.] The term ''correlation peaks'' is preferred since it indicates the mechanism by which these extra features arise. In some cases[4–6] correlation effects are so severe that distinguishing the main or parent peak from the satellite peaks is not possible. Thus the term ''satellite'' will be inconsistent in these cases.

The advent of dedicated synchrotron radiation sources has improved the experimental investigation of correlation peaks by allowing higher energy resolution photoelectron spectra of atoms and molecules to be taken. Since correlation effects are seen to be stronger in the inner valence and core regions of the photoelectron spectrum, traditional photon sources of high energy resolution (e.g., HeI, 21.2 eV) cannot be used. On the other hand, higher energy photon sources such as discrete x-rays are only capable of energy resolutions greater than ≈0.80 eV FWHM. The high brightness, variable photon energy, and high energy resolution provided by the so-called second generation synchrotron sources are perfectly suited for the detailed investigation of correlation peaks. For example, in the present synchrotron PES experiment (32–72 eV photon energy), the total experimental energy resolution of ≤0.40 eV FWHM is routinely obtained. With these new instrumental capabilities the mechanisms that give rise to correlation peaks can be classified, for example, in the phenomenological scheme of Becker and Shirley.[7]

Acetylene, with a ground state electronic configuration $(^1\Sigma_g^+)$

$$C_2H_2(D_{\infty h}):(1\sigma_g)^2(1\sigma_u)^2(2\sigma_g)^2(2\sigma_u)^2(3\sigma_g)^2(1\pi_u)^4$$

has been of particular interest due to its simple structure, numerous applications, and very rich inner valence region in terms of correlation effects. Dixon *et al.*[8] observed significant satellite structure in the inner valence region of C_2H_2 using binary $(e,2e)$ spectroscopy and considered these structures to be associated with the $2\sigma_g^{-1}$ ionization process $(^2\Sigma_g^+)$. On the other hand, Cavell and Allison[9] considered

[a)]Author to whom correspondence should be addressed.

Downloaded 11 Dec 2003 to 137.82.31.98. Redistribution subject to AIP license or copyright, see http://ojps.aip.org/jcpo/jcpcr.jsp

the 27.5 eV satellite to be associated with the $2\sigma_u^{-1}$ ionization process ($^2\Sigma_u^+$) on the basis of discrete x-ray photoelectron spectroscopy experiments. These earlier studies were followed by extensive investigations using different experimental and theoretical techniques.[10–24]

Later better-resolved PES experimental studies resolved the broad satellite at 27.5 eV into two correlation (satellite) peaks at 26.7 and 28.0 eV.[11] Theoretical calculations of Cederbaum *et al.*[13] and Bradshaw *et al.*[14] predicted a $^2\Sigma_g^+$ assignment for both correlation peaks. Furthermore, interference effects between the $2\sigma_g^{-1}$ and $3\sigma_g^{-1}$ processes were suggested as an explanation for the variations in the satellite/main intensity ratio as a function of photon energy.

A more recent PES study using monochromatic x-ray by Svensson *et al.*[15] resolved five correlation peaks (numbered 1–5 in order of increasing binding energy). [A similar numbering scheme is adopted in the present work: satellite 1 (26.6 eV), satellite 2 (28.0 eV), satellite 3 (29.8 eV), and satellite 4 (31.2 eV).] Since then, various theoretical and experimental attempts have provided widely different interpretations as to the symmetry assignment of these correlation peaks. To mention a few, Chong[16] has considered $^2\Sigma_u^+$ symmetry for satellite 2 and $^2\Sigma_g^+$ symmetry for satellites 1 and 3, while Wasada and Hirao[17] have assigned $^2\Sigma_u^+$ for satellites 1 and 2 and $^2\Sigma_g^+$ symmetry for satellites 3 and 4 on the basis of theoretical calculations. More recently, Koch *et al.*[18] assigned $^2\Sigma_u^+$ symmetry for satellite 1 and $^2\Sigma_g^+$ for satellites 2 and 4 on the basis of synchrotron PES experiments. Weigold *et al.*[19] and Duffy *et al.*[20] assigned the symmetries of all the satellites (1–4) to $^2\Sigma_g^+$ on the basis of electron momentum spectroscopy (EMS) experiments.

In this work, we present a high resolution ($\leqslant$0.40 eV FWHM) synchrotron PES work along with multireference singles and doubles configuration interaction (MRSDCI) calculations in an effort to assign the correct symmetry as well as to understand the nature of the mechanisms giving rise to these correlation (satellite) peaks. This is the first study of the valence photoelectron spectrum of acetylene to include both experimental and theoretical results with semiquantitative agreement in terms of the binding energies and the relative ionization intensities.

II. EXPERIMENTAL METHOD

The synchrotron PES spectra of acetylene for a range of photon energies from 32 to 72 eV were obtained at the 3m-TGM beamline at the Synchrotron Radiation Center (University of Wisconsin) using the Canadian Synchrotron Radiation Facility (CSRF) Mcpherson photoelectron spectrometer.[25] A thin aluminum window isolated the spectrometer from the beamline and also removed higher order radiation. Both the high energy grating (HEG) and low energy grating (LEG) of the 3m-TGM are utilized in the experiments. No angular corrections to the derived cross sections were necessary since the photoelectrons were collected at the psuedomagic angle. All reported photoelectron intensity ratios were corrected for transmission effects.[26] The total experimental energy resolution (electron energy analyzer and monochromator) for these experiments was about 0.40 eV FWHM. A research purity sample of acetylene (99.9%) was supplied by Matheson Gas Products and 1,2-^{13}C–acetylene (99%) was supplied by Isotec Inc.

III. THEORETICAL DETAILS

Within the framework of the dipole approximation, the photoionization transition amplitude (μ_j) is given by

$$\mu_j = \langle \Psi_j(N-1)\chi^j(k)|\mu|\Psi(N)\rangle, \tag{1}$$

where $\Psi(N)$ is the ground state N-electron wave function, $\Psi_j(N-1)$ is the jth ionic state wave function, μ is the dipole operator, and $\chi^j(k)$ is the continuum function for the outgoing photoelectron with momentum k and associated with state j. Here, $\Psi(N)$ and $\Psi_j(N-1)$ are written as linear combinations of all possible configurations. This is referred to as the configuration interaction (Cl) picture. The transition amplitude can also be written as,

$$\mu_j = \langle \chi^j(k)|\mu|\varphi^j_{\text{Dyson}}\rangle S_j, \tag{2}$$

where φ^j_{Dyson} is the Dyson orbital[27,28] and S_j^2 is the so-called pole strength or the ionization probability for the jth ionic state. The pole strength for the jth ionic state is defined as

$$S_j^2 = \|\langle \Psi_j(N-1)|\Psi(N)\rangle_{N-1}\|^2, \tag{3}$$

where the integration is performed over $N-1$ electrons.

In practice, PES measurements are taken at a fixed photon energy and the intensity ratio of the correlation (satellite) peak relative to a primary peak with a similar Dyson orbital is obtained. In this case, the intensity ratio of the jth correlation peak to the pth primary peak of the same symmetry (and under certain conditions) is given by the familiar expression,[27,28]

$$\frac{I(j)}{I(p)} \approx \frac{S_j^2}{S_p^2}. \tag{4}$$

This approximation is only valid whenever the dipole matrix elements ($\langle \chi^j(k)|\mu|\phi^j_{\text{Dyson}}\rangle$) for the jth correlation peak and the pth primary peak are nearly equal. Furthermore, coupling of channels in the continuum is neglected; that is, conjugate shake-up processes are assumed to be negligible. In the present approximation, the explicit form of the continuum function ($\chi^j(k)$) is not specified. It is only assumed that the continuum functions for state j and state p are similar. More accurate calculations (beyond that employed in the present study) will definitely include explicit calculations of the continuum functions such as those employed by McKoy *et al.*[29] and Lucchese *et al.*[30] Combining the present type of MRSDCI calculations with explicit continuum state calculations is not feasible with current computer hardware and software technology.

Typically, the primary peak can be represented by a single hole configuration ($0p-1h$) and thus S_p^2 is close to unity. The pole strength for the jth correlation peak is usually much smaller ($S_j^2 \ll 1$) and qualitatively describes the probability of finding the ($0p-1h$) configuration in the jth correlation state. This results from the well known spectroscopic factor (pole strength) sum rules, $\Sigma_k S_k^2 = 1$.

Downloaded¬11¬Dec¬2003¬to¬137.82.31.98. Redistribution subject to AIP license or copyright,¬see¬http://ojps.aip.org/jcpo/jcpcr.jsp

In order to understand the origin and symmetry of these correlation states, a series of theoretical calculations of the photoelectron spectrum of acetylene using a 171-CGTO basis set was performed. The $(18s\ 13p)$ Partridge basis set[31] was chosen as the primitive basis for carbon. For hydrogen, Partridge's $(10s)$ basis[32] was used. For carbon, the first 14 s functions were contracted into two s functions using the $1s$ and $2s$ atomic orbital coefficients. Similarly, the first seven p functions were contracted into one p function using the $2p$ atomic orbital coefficients. For hydrogen, the first six s functions were contracted into one s function using the $1s$ atomic orbital coefficients. The rest of the functions were left uncontracted. This scheme lost less than 0.1 kcal/mol in a trial SCF calculation on CH_4.[33] All of the polarization functions were taken from Dunning.[34] For carbon, $(3d1f)$ $(\alpha_d=1.848,$ 0.649, 0.228, $\alpha_f=0.761)$ polarization functions were used; for hydrogen, $(2p1d)$ $(\alpha_p=1.257,$ 0.355, $\alpha_d=0.916)$ were used. This basis was further augmented by putting three p and three d diffuse Rydberg functions on the center of the C–C bond with exponents of 0.026, 0.052, and 0.104 for both p and d functions. All Cartesian components were kept for d and f functions. Therefore, the final basis set was $[6s7p3d1f/5s2p1d]$ ++++++, or 171-CGTO in short. This basis set without the most diffuse Rydberg $3p$ and $3d$ functions has been used in recent theoretical calculations on ethylene.[27,28]

To keep the results directly comparable with earlier work on acetylene, $D_{\infty h}$ geometry was used with $R(\mathrm{CC})=1.203$ Å, $R(\mathrm{CH})=1.061$ Å. An SCF calculation was done for the ground state configuration with D_{2h} point group symmetry constraints and orbital labeling, $(1a_g)^2(1b_{1u})^2(2a_g)^2(2b_{1u})^2(3a_g)^2(1b_{2u})^2(1b_{3u})^2$. This allowed the computer program to exploit the simplifications that come from the D_{2h} subgroup of the full group. The calculated SCF total energy for the ground state is $-76.855\,08$ hartree. For each irreducible representation of the radical cation, a multireference singles and doubles configuration interaction (MRSDCI) calculation based on improved virtual orbitals (IVO)[35] is performed. The theoretical binding energy spectrum based on this calculation did not compare well with the experimental PES spectrum especially at the high-energy region from 20 to 35 eV. To obtain better results, frozen average natural orbitals (FANO) were employed. From the MRSDCI-IVO calculation results, the first 40 roots of each irreducible representation are included in the average (density matrix) for each irreducible representation. Then, MRSDCI calculations based on FANO's were done for each irreducible representation of the radical cation. This theoretical calculation is hereafter referred to as the MRSDCI(ANO) calculation and further computational details are available.[36] The energy levels have been shifted so that the primary peaks of each irreducible representation agree with the experimental primary hole positions[12,37] to avoid the problem of getting the neutral and ionized molecule states to the same accuracy.

IV. RESULTS AND DISCUSSION

A high resolution photoelectron spectrum of acetylene (at 68.8 eV photon energy) containing the main $2\sigma_g^{-1}$ peak and four correlation (satellite) peaks with binding energies of 23.5, 26.6, 28.0, 29.8, and 31.2 eV, respectively is presented in Fig. 1(a). The deconvolution of the photoelectron spectrum of acetylene involved an assumption made by Svensson *et al.*[15] using AlKα XPS that there are two correlation peaks (peaks 3 and 4) in the binding energy range 29–32 eV. Our present experiments do not resolve correlation peaks 3 and 4 clearly; however, the peak width and energy assignments are made consistent with those of Svensson *et al.*[15] The energy scale was calibrated by aligning the main $2\sigma_g^{-1}$ peak to the well-known binding energy of the $2\sigma_g$ orbital obtained from high resolution He II spectrum.[37] Additional Gaussian peaks to the high and low energy side of the $2\sigma_g^{-1}$ main peak were fitted to account for its broad structure. Single Gaussian peaks are fitted to correlation peaks 1–4 with widths 0.51, 0.51, 0.85, and 0.85 eV FWHM, respectively. The width of the $2\sigma_g^{-1}$ main peak is 0.44 eV FWHM with additional peaks (of the same width) on either side of the main peak to represent the broad structure. It should be noted that even higher energy resolution PES spectra ($\approx$0.3 eV FWHM) do not resolve any new structures. The observed experimental widths are very close to the natural widths; this is consistent with the fact that these inner valence states are largely dissociative states.

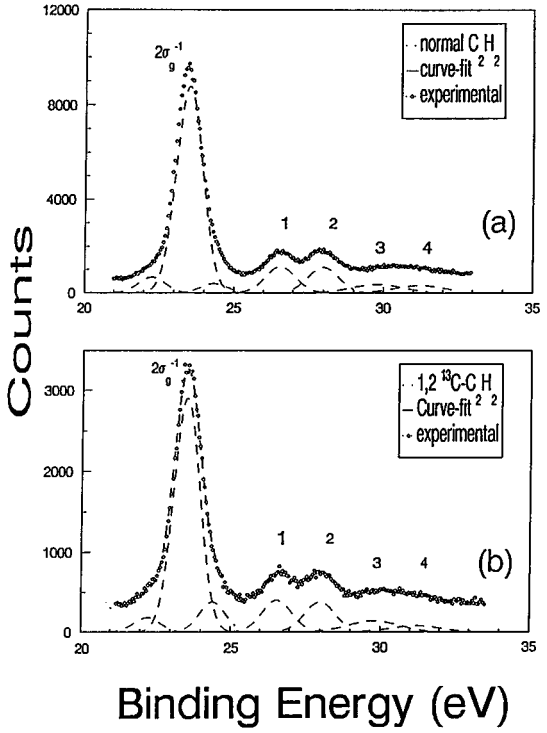

FIG. 1. A representative photoelectron spectrum of acetylene and isotopically labeled acetylene taken at photon energy of 68.8 eV (a) and 72.4 eV (b) with a total energy resolution of 0.40 eV FWHM. The spectrum as shown is not corrected for transmission effects. Gaussian curves are fitted to the correlation peaks (satellites 1–4) and the $2\sigma_g^{-1}$ main peak. The $1\pi_u^{-1}$ (11.43 eV binding energy), $3\sigma_g^{-1}$ (16.7 eV binding energy) and $2\sigma_u^{-1}$ (18.78 eV binding energy) main peaks are not shown.

To investigate whether these correlation peaks are of purely ''electronic'' origins, a PES spectrum of isotopically labeled acetylene (1,2-^{13}C–C_2H_2) was obtained as shown in

Downloaded¬11¬Dec¬2003¬to¬137.82.31.98. Redistribution subject to AIP license or copyright,¬see¬http://ojps.aip.org/jcpo/jcpcr.jsp

TABLE I. Transmission-corrected intensity ratios[a] of satellite peaks[b] to $2\sigma_g^{-1}$ for the spectra of normal acetylene obtained with high energy grating (HEG).

$h\nu$	sat.1 ($\pm\sigma$)	sat.2 ($\pm\sigma$)	sat.3 ($\pm\sigma$)	sat.4 ($\pm\sigma$)
44	0.152 (0.011)	0.155 (0.014)	0.164 (0.022)	0.183 (0.034)
45	0.075 (0.023)	0.078 (0.024)	0.111 (0.019)	0.118 (0.040)
48	0.085 (0.010)	0.094 (0.011)	0.010 (0.016)	0.070 (0.025)
50	0.081 (0.010)	0.101 (0.009)	0.026 (0.014)	0.100 (0.015)
52	0.102 (0.008)	0.125 (0.009)	0.057 (0.014)	0.098 (0.021)
56	0.112 (0.010)	0.133 (0.010)	0.068 (0.014)	0.086 (0.015)
60	0.118 (0.005)	0.131 (0.005)	0.070 (0.008)	0.065 (0.009)
62	0.119 (0.007)	0.132 (0.007)	0.067 (0.010)	0.068 (0.010)
64	0.121 (0.009)	0.131 (0.009)	0.066 (0.013)	0.065 (0.013)
68	0.129 (0.042)	0.137 (0.006)	0.070 (0.008)	0.060 (0.009)
70	0.134 (0.009)	0.137 (0.009)	0.072 (0.009)	0.057 (0.008)
72	0.145 (0.006)	0.138 (0.006)	0.084 (0.009)	0.062 (0.010)

[a]The quoted error limits are statistical errors and do not include systematic errors which are estimated to be $\leqslant$10%.
[b]The binding energies of the satellite peaks 1–4 are 26.56, 28.0, 29.79, 31.2 eV, respectively.

Fig. 1(b). No significant difference in terms of binding energy, peak widths, or peak areas of any of the ionization peaks was observed between acetylene and ^{13}C-labeled acetylene. The binding energy spectrum (Fig. 1) along with the photon energy dependence study of correlation peak intensity ratios (presented later) indicate that the correlation peaks are not influenced by extraneous electron–nuclear scattering processes.

A similar study of the photoelectron spectrum of ethylene and ^{13}C-labeled ethylene also has shown no observable differences.[27] Taken together, the PES results for ethylene, acetylene, and their ^{13}C-substituted analogues are strongly supportive of the idea that correlation peaks are of purely ''electronic'' origin.

To address the controversy surrounding the symmetry assignment of these correlation peaks, a study of the photon energy dependence of the intensity ratios of the correlation peaks relative to the $2\sigma_g^{-1}$ main peak was performed. The results are presented in Tables I–III and shown in Fig. 2 for C_2H_2 and in Fig. 3 for 1,2 ^{13}C–C_2H_2. Note that the results are almost identical; there is no significant difference in

TABLE II. Transmission-corrected intensity ratios[a] of satellite peaks[b] to $2\sigma_g^{-1}$ for spectra of normal acetylene obtained with low energy grating (LEG).

$h\nu$	sat.1 ($\pm\sigma$)	sat.2 ($\pm\sigma$)	sat.3 ($\pm\sigma$)	sat.4 ($\pm\sigma$)
42	0.156 (0.011)	0.149 (0.011)	0.154 (0.015)	0.274 (0.019)
44	0.092 (0.019)	0.096 (0.020)	0.071 (0.034)	0.118 (0.033)
46	0.183 (0.107)	0.168 (0.012)	0.145 (0.019)	0.114 (0.024)
48	0.132 (0.012)	0.133 (0.012)	0.103 (0.021)	0.093 (0.020)
50	0.115 (0.008)	0.127 (0.007)	0.068 (0.011)	0.084 (0.013)
52	0.126 (0.007)	0.138 (0.007)	0.084 (0.011)	0.098 (0.010)
54	0.109 (0.045)	0.130 (0.048)	0.063 (0.009)	0.082 (0.010)
56	0.113 (0.049)	0.146 (0.018)	0.127 (0.023)	0.018 (0.020)

[a]The quoted error limits are statistical errors and do not include systematic errors which are estimated to be $\leqslant$10%.
[b]The binding energies of the satellite peaks 1–4 are 26.56, 28.00, 29.79, and 31.2 eV, respectively.

TABLE III. Transmission-corrected intensity ratios[a] of satellite peaks[b] to $2\sigma_g^{-1}$ for the spectra of labeled acetylene obtained with low energy grating (LEG).

$h\nu$	sat.1 ($\pm\sigma$)	sat.2 ($\pm\sigma$)	sat.3 ($\pm\sigma$)	sat.4 ($\pm\sigma$)
42	0.089 (0.009)	0.085 (0.010)	0.040 (0.017)	0.354 (0.019)
46	0.141 (0.016)	0.158 (0.016)	0.063 (0.025)	0.155 (0.029)
48	0.095 (0.009)	0.103 (0.010)	0.020 (0.017)	0.058 (0.018)
50	0.112 (0.007)	0.119 (0.007)	0.053 (0.012)	0.079 (0.012)
52	0.106 (0.008)	0.118 (0.007)	0.056 (0.011)	0.081 (0.011)
56	0.114 (0.007)	0.121 (0.007)	0.053 (0.010)	0.099 (0.011)
60	0.131 (0.006)	0.126 (0.007)	0.055 (0.010)	0.077 (0.010)
62	0.132 (0.006)	0.136 (0.006)	0.069 (0.010)	0.079 (0.010)
68	0.136 (0.005)	0.143 (0.006)	0.075 (0.009)	0.081 (0.009)
70	0.141 (0.006)	0.147 (0.006)	0.074 (0.001)	0.079 (0.010)
70.4	0.143 (0.005)	0.145 (0.005)	0.074 (0.007)	0.067 (0.008)
72	0.143 (0.004)	0.141 (0.004)	0.060 (0.004)	0.060 (0.007)
72.5	0.146 (0.010)	0.129 (0.011)	0.026 (0.016)	0.116 (0.016)
73.5	0.151 (0.008)	0.146 (0.008)	0.112 (0.012)	0.075 (0.013)

[a]The quoted error limits are statistical errors and do not include systematic errors which are estimated to be $\leqslant$10%.
[b]The binding energies of the satellite peaks 1–4 are 26.56, 28.0, 29.79, and 31.2 eV, respectively.

the correlation peak to main $2\sigma_g^{-1}$ peak intensity ratios observed for normal C_2H_2 and 1,2 ^{13}C–C_2H_2. This is further assurance that correlation peaks in acetylene are independent of electron–nuclear scattering effects.

It can be seen (Figs. 2 and 3) that satellites 1, 2, and 3 show relatively constant intensity ratios with respect to the main $2\sigma_g^{-1}$ peak, while satellite 4 exhibits an increase in intensity ratio with respect to the main $2\sigma_g$ peak as threshold (31.2 eV) is approached. In fact, all these correlation (satellite) peaks show constant photon energy dependence in the 50–75 eV range, with some variations at the lower photon

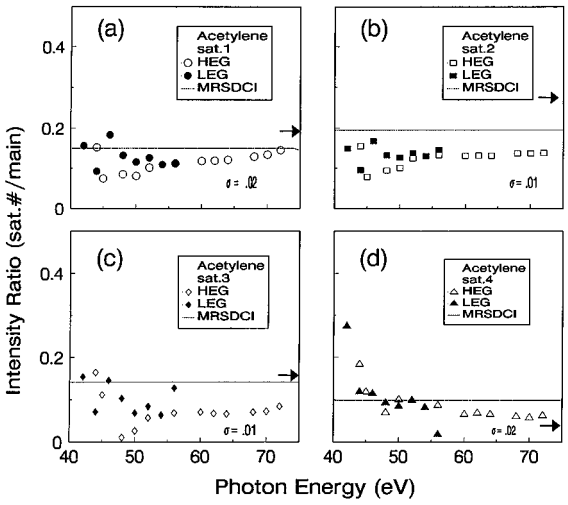

FIG. 2. Normal acetylene: photon energy dependence of the intensity ratio of (a) satellite 1, (b) satellite 2, (c) satellite 3, and (d) satellite 4 at binding energies of 26.56, 28.0, 29.79, and 31.2 eV, respectively. The intensity ratios are taken with respect to $2\sigma_g^{-1}$ main peak at binding energy of 23.51 eV. All reported intensity ratios are corrected for transmission effects. The corresponding XPS values (Ref. 15) are indicated by an arrow. The MRSDCI value was obtained by summing all pole strengths in the respective satellite regions and dividing by the pole strength in 22–24 eV (see Table IV).

Downloaded¬11¬Dec¬2003¬to¬137.82.31.98. Redistribution¬subject¬to¬AIP¬license¬or¬copyright,¬see¬http://ojps.aip.org/jcpo/jcpcr.jsp

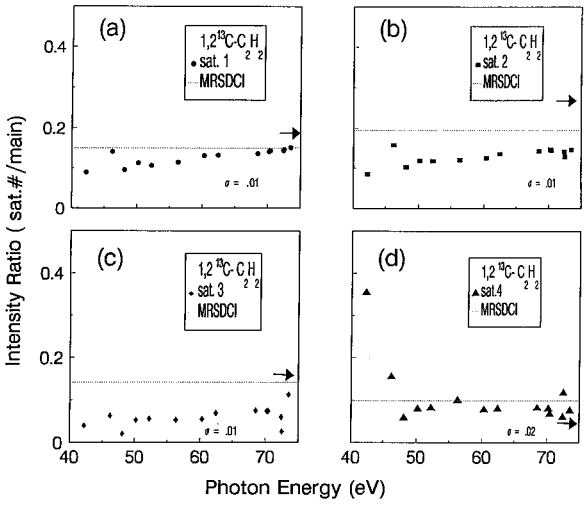

FIG. 3. Isotopically labeled acetylene: photon energy dependence of the intensity ratio of (a) satellite 1, (b) satellite 2, (c) satellite 3, and (d) satellite 4, respectively, at binding energies of 26.56, 28.0, 29.79, and 31.2 eV. The intensity ratios are taken relative to the $2\sigma_g^{-1}$ main peak at binding energy of 23.51 eV. All reported intensity ratios are corrected for transmission effects. The corresponding XPS values (Ref. 15) are indicated by an arrow. The MRSDCI value was obtained by summing all the pole strengths in the respective satellite regions and dividing by the pole strengths in 22–24 eV (see Table IV).

energies (40–50 eV). The constant photon energy dependence is consistent with a predominantly $^2\Sigma_g^+$ symmetry assignment to these four correlation peaks; as correlation peaks which derive their intensity from different symmetry orbitals show strong variations in their intensity ratio with respect to one of the main peaks. Since the experimentally determined $1\pi_u/2\sigma_g$ main peak and $3\sigma_g/2\sigma_g$ main peak ratios[10] as well as the $2\sigma_u/2\sigma_g$ main peak ratios[38] show a smooth decrease with increasing photon energy in the range 40–75 eV, we can use the correlation peak to $2\sigma_g^{-1}$ main peak intensity ratios for distinguishing the major contributor to a particular correlation peak. This is particularly true if there are contributions from ionic states with significant carbon $2p$ character such as $^2\Pi_u$ since the variations of the $1\pi_u/2\sigma_g$ main peak intensity ratio are very substantial. The variations in the $2\sigma_u/2\sigma_g$ main peaks are relatively smaller and the intensity ratio is constant in the photon energy range 55–75 eV. The photon energy dependence studies of the correlation peak to $2\sigma_g^{-1}$ as well as to $3\sigma_g^{-1}$ main peak intensity ratios which indicate predominantly $^2\Sigma_g^+$ symmetry are supported by MRSDCI calculations (see later section).

The present symmetry assignment ($^2\Sigma_g^+$) is also consistent with recent electron momentum spectroscopy (EMS) experiments.[19,20] The experimental momentum profiles for the correlation peaks measured by Weigold *et al.*[19] and Duffy *et al.*[20] indicate that most of the intensity of these correlation peaks are associated with the $2\sigma_g^{-1}$ process (i.e., $^2\Sigma_g^+$). However, it should be noted that the EMS measurements are done at an energy resolution of $\geqslant$1.5 eV FWHM which is significantly poorer than the energy resolution of synchrotron PES measurements ($\leqslant$0.4 eV FWHM). EMS measurements provide direct symmetry information whereas variable photon energy synchrotron PES measurements are more of an indirect method. Thus synchrotron PES (a noncoincident technique) and EMS (a coincident technique) are complementary experimental tools for elucidating the symmetry of correlation (satellite) peaks.

The slight variations in the intensity ratio of satellites 1–3 in the 40–50 eV range can be due to a number of reasons. Close to threshold, autoionization (interchannel coupling) from doubly excited states introduces resonance structures in the photon energy dependence of correlation state cross sections.[39,40] A doubly excited state of a neutral molecule (M^{**}) contains two electrons excited to higher bound energy levels. This doubly excited neutral state can lose an electron (i.e., autoionize) leading to different excited states of the ion (M^{+*}) which we refer to as the correlation (satellite) states. Thus observation of the correlation state cross sections as a function of exciting photon energy will show sharp resonance structures corresponding to the energies of doubly excited states of the neutral. Since the photon energy spacings between the present measurements are $\geqslant$2 eV, the resonance fine structures cannot be observed; instead a scatter of data points can be seen in the 40–50 eV photon energy range (Figs. 2 and 3). Another factor contributing to these variations is the experimental PES background. At low photon energies, especially below 40 eV, the sloping background prevents very accurate determination of intensity ratios. These errors are listed in Tables I–III and shown in Figs. 2 and 3. It can be seen that the observed variations are much larger than the error limits (1σ) of the intensity ratios. This indicates that these variations may be largely due to autoionization resonance structures yet to be identified.

It is worthwhile to note that the satellite/main $2\sigma_g^{-1}$ peak intensity ratios for satellites 1–3 (Figs. 2 and 3) are consistently lower than those obtained from the x-ray photoelectron (XPS) spectrum (at 1487 eV) of Svensson *et al.*[15] The XPS values of Svensson *et al.* are indicated by a horizontal arrow in Figs. 2 and 3. The discrepancy between the present measurements and the XPS values may be a real effect and can only be ascertained by performing synchrotron PES measurements at photon energies greater than 80 up to 1487 eV. However, it is most likely that the discrepencies are due to higher atomic photoionization cross section of C_{2s} orbital compared to C_{2p} orbitals at higher photon energies (i.e., x-ray energies). At $\approx$1487 eV photon energy, photoionization cross section of C_{2s} orbital is 66 times larger than that of C_{2p} orbital.[41] This significant difference between the photoionization cross section of C_{2s} and C_{2p} orbitals gives rise to higher intensity of those satellites which are of symmetries with mostly C_{2s} character and lower intensity of those satellites which are of symmetries with more C_{2p} character. Since the main $2\sigma_g^{-1}$ peak has some $1\pi_u^{-1}$ poles as shown in the MRSDCI calculations (see later section), there is some C_{2p} character in the main $2\sigma_g^{-1}$ peak. Satellites 1 and 4 are also predicted to have contributions from symmetry orbitals with strong C_{2p} character ($1\pi_u$ and $3\sigma_g$) thus the sat.$1/2\sigma_g$ and sat.$4/2\sigma_g$ intensity ratios at 50–75 eV are similar to the corresponding ratios at 1487 eV. In contrast, satellite 2 is of pure $2\sigma_g$ symmetry whereas satellite 3 has $2\sigma_g$ and $2\sigma_u$ symmetry which are all symmetry orbitals with strong C_{2s} character. Therefore, the sat.$2/2\sigma_g$ and sat.$3/2\sigma_g$ intensity

Downloaded¬11¬Dec¬2003¬to¬137.82.31.98. Redistribution subject to AIP license or copyright,¬see¬http://ojps.aip.org/jcpo/jcpcr.jsp

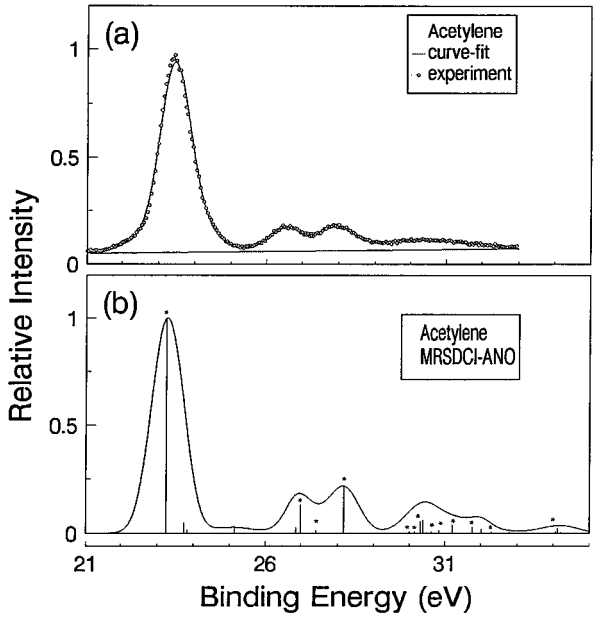

FIG. 4. Comparison of the experimental binding energy spectrum (a) of acetylene with the theoretical spectrum (b) based on MRSDCI(ANO) calculation using a 171-CGTO basis set. The calculated pole strengths (solid poles) are convoluted with the experimental peak widths to yield the curve (solid line) which can be compared with the experiment (b). Poles associated mainly with the $2\sigma_g^{-1}$ and $3\sigma_g^{-1}$ ionization processes are labeled with a star. (see Table IV).

ratios at 50–75 eV are lower than the corresponding ratios at 1487 eV. The C_{2s} and C_{2p} contributions provide a consistent explanation for the similarities as well as differences between the intensity ratios observed in the present experiment and those observed by Svensson *et al.*[15] at 1487 eV.

Current interest in photon energy dependence of intensity ratios lies mostly in understanding the different mechanisms giving rise to these correlation peaks. Using the classification scheme of Becker and Shirley,[7] satellites 1, 2, and 3 can be regarded as intrinsic and satellite 4 as dynamic on the assumption that all peaks (1, 2, 3, and 4) are largely associated with the $2\sigma_g^{-1}$ ionization process. Intrinsic correlation (satellite) peaks are those whose intensity is independent of the photon energy while dynamic correlation (satellite) peaks are those whose intensity depends on photon energy. The sudden increase in intensity ratio of satellite 4 near threshold may be explained by assuming that it is of dynamic type, i.e., one whose intensity changes with photon energy. This is obviously clear even though there are few data points since the trend is observed consistently in normal acetylene [Fig. 2(d)] and labelled acetylene [Fig. 3(d)]. The trend of increasing cross section of satellite 4 as threshold is approached is consistent with a conjugate shake-up process[42] and has been observed in many atomic[43–46] and molecular[47] systems.

An alternative and more plausible explanation can be advanced for the photon energy dependence of the sat.$4/2\sigma_g$ intensity ratio. The theoretical PES of acetylene obtained from the MRSDCI(ANO) calculations is shown in Fig. 4 and Table IV. It can be seen that satellite 4 is composed primarily of $^2\Sigma_g$ correlation states. However, two of the correlation states (31.15 and 31.66 eV binding energy) corresponding to satellite 4 are associated with the $3\sigma_g^{-1}$ ionization process as opposed to the usual $2\sigma_g^{-1}$ ionization process (see Table IV); both of these processes have overall $^2\Sigma_g$ symmetry. The 31.15 eV state has a normalized Dyson orbital that is approximately $0.8(2\sigma_g)+0.6(3\sigma_g)$ whereas the 31.66 eV state has a normalized Dyson orbital that is nearly pure $3\sigma_g$. Since the $3\sigma_g$ molecular orbital contains significant C_{2p} character, the $3\sigma_g/2\sigma_g$ main peak ratio will decrease as the photon energy increases. The same trend is observed experimentally for sat.$4/2\sigma_g$ main peak (see Figs. 2 and 3) which strongly suggests that sat.$4/3\sigma_g$ main peak intensity ratio is constant with increasing photon energy. The photon energy dependence of the sat.$4/3\sigma_g$ main peak intensity ratio is shown in Fig. 5 in comparison with the predicted MRSDCI pole strength ratio. The present intensity ratios (Fig. 5) were obtained using additional experimental PES data for the $2\sigma_g/3\sigma_g$ main peak ratio. The photon energy dependence curve is clearly constant in the photon energy range 45–75 eV. Very good agreement with the predicted MRSDCI ratio is also obtained.

Although the correlation states at 31.15 and 31.66 eV are only 2 of 4 other states in the satellite 4 binding energy region, on the basis of their relative pole strengths it can be said that the observed photon energy dependence of satellite 4 is associated mainly with the $3\sigma_g^{-1}$ ionization process rather than being a ''dynamic'' correlation state associated with the $2\sigma_g^{-1}$ ionization process. It should be noted that this possibility (i.e., interference of $3\sigma_g^{-1}$ and $2\sigma_g^{-1}$ ionization processes in $^2\Sigma_g$ correlation states) was first suggested by Bradshaw *et al.*;[10] however, it was made in relation to satellite 1 and not to satellite 4. This explanation is in variance with some of the conclusions made in the recent EMS studies of Weigold *et al.*[19] and Duffy *et al.*[20] Careful examination of the original EMS results indicate that the predominant assignment of $2\sigma_g^{-1}$ poles to satellite 4 was based on spectroscopic factor measurements of the $3\sigma_g^{-1}$ main peak. EMS spectroscopic factor measurements for the $3\sigma_g^{-1}$ main peak indicate the same spectroscopic factor as the spectroscopic factor for the $1\pi_u^{-1}$ main peak which was assumed to be approximately one (ignoring degeneracy). The EMS assumption is clearly inconsistent with the present MRSDCI calculations which predict significant splitting of the main $3\sigma_g$ and $1\pi_u$ poles with $^2\Pi_u$ correlation states predicted at 26.86 and 32.02 eV and $^2\Sigma_g$ correlations states associated with $3\sigma_g^{-1}$ ionization process predicted at 31.15 and 31.66 eV. The calculated $3\sigma_g^{-1}$ pole strengths in the satellite 4 binding energy region are small but not insignificant ($\approx$0.03) and are in fact observable in the present synchrotron PES experiments. Note that the predicted $^2\Pi_u$ correlation state at 26.86 eV is consistent with the value of the sat.$1/2\sigma_g$ main intensity ratio (see above) relative to the corresponding intensity ratio at x-ray energies. Thus the EMS assumptions that the main $3\sigma_g^{-1}$ and main $1\pi_u^{-1}$ pole strengths are one, although reasonable since these are outer valence orbitals, may be incorrect.

A stronger argument for assigning peak 4 to the $3\sigma_g^{-1}$ process as opposed to the $2\sigma_g^{-1}$ process is perhaps in the measured momentum distributions. Examination of the origi-

Downloaded¬11¬Dec¬2003¬to¬137.82.31.98. Redistribution subject to AIP license or copyright,¬see¬http://ojps.aip.org/jcpo/jcpcr.jsp

TABLE IV. The calculated line positions and intensities for the PES of acetylene.[a]

Symmetry	Ionization energy (eV)[d]	Intensity[b] (S_j^2)	Important configurations[c]
$^2\Sigma_g^+$	16.36	0.797	0.90 $(3\sigma_g)^{-1}$
			0.19 $(2\sigma_u)^{-1}$ $(1\pi_u)^{-1}$ $(1\pi_g)^1$
			0.19 $(3\sigma_g)^{-1}$ $(1\pi_u)^{-1}$ $(n\pi_u)^1$
			0.18 $(3\sigma_g)^{-1}$ $(1\pi_u)^{-2}$ $(1\pi_g)^2$
	23.17	0.519	0.72 $(2\sigma_g)^{-1}$
			0.48 $(2\sigma_u)^{-1}$ $(1\pi_u)^{-1}$ $(1\pi_g)^1$
			0.17 $(2\sigma_g)^{-1}$ $(1\pi_u)^{-1}$ $(n\pi_u)^1$
			0.16 $(1\pi_u)^{-2}$ $(n\sigma_g)^1$
			0.16 $(1\pi_u)^{-2}$ $(n\delta_g)^1$
			0.15 $(2\sigma_g)^{-1}$ $(1\pi_u)^{-2}$ $(1\pi_g)^2$
			0.11 $(3\sigma_g)^{-1}$ $(1\pi_u)^{-2}$ $(1\pi_g)^2$
	26.93	0.061	0.61 $(1\pi_u)^{-2}$ $(n\delta_g)^1$
			0.51 $(2\sigma_u)^{-1}$ $(1\pi_u)^{-1}$ $(1\pi_g)^1$
			0.32 $(1\pi_u)^{-2}$ $(n\sigma_g)^1$
			0.25 $(2\sigma_g)^{-1}$
			0.19 $(3\sigma_g)^{-1}$ $(1\pi_u)^{-2}$ $(1\pi_g)^2$
	27.34	0.010	0.88 $(1\pi_u)^{-2}$ $(n\delta_g)^1$
			0.17 $(2\sigma_u)^{-1}$ $(1\pi_u)^{-1}$ $(1\pi_g)^1$
			0.10 $(2\sigma_g)^{-1}$
	28.13	0.112	0.72 $(1\pi_u)^{-2}$ $(n\delta_g)^1$
			0.39 $(2\sigma_u)^{-1}$ $(1\pi_u)^{-1}$ $(1\pi_g)^1$
			0.34 $(2\sigma_g)^{-1}$
			0.16 $(3\sigma_g)^{-1}$ $(1\pi_u)^{-2}$ $(1\pi_g)^2$
	30.09	0.005	0.87 $(1\pi_u)^{-2}$ $(n\sigma_g)^1$
			0.15 $(3\sigma_g)^{-1}$ $(1\pi_u)^{-2}$ $(n\sigma_g)^1$ $(n\delta_g)^1$
			0.13 $(2\sigma_u)^{-1}$ $(1\pi_u)^{-2}$ $(n\sigma_u)^1$ $(n\delta_g)^1$
			0.09 $(3\sigma_g)^{-1}$ $(1\pi_u)^{-2}$ $(1\pi_g)^2$
			0.07 $(2\sigma_g)^{-1}$
	30.29	0.034	0.53 $(3\sigma_g)^{-1}$ $(1\pi_u)^{-2}$ $(1\pi_g)^2$
			0.38 $(2\sigma_u)^{-1}$ $(1\pi_u)^{-1}$ $(1\pi_g)^1$
			0.36 $(1\pi_u)^{-2}$ $(n\sigma_g)^1$
			0.34 $(1\pi_u)^{-2}$ $(n\delta_g)^1$
			0.31 $(3\sigma_g)^{-1}$ $(1\pi_u)^{-1}$ $(1\pi_g)^1$
			0.17 $(2\sigma_g)^{-1}$
	30.55	0.005	0.59 $(1\pi_u)^{-2}$ $(n\delta_g)^1$
			0.49 $(3\sigma_g)^{-1}$ $(1\pi_u)^{-2}$ $(1\pi_g)^2$
			0.38 $(1\pi_u)^{-2}$ $(n\sigma_g)^1$
			0.06 $(2\sigma_g)^{-1}$
			0.06 $(3\sigma_g)^{-1}$
	30.77	0.008	0.81 $(3\sigma_g)^{-1}$ $(1\pi_u)^{-1}$ $(n\pi_u)^1$
			0.31 $(3\sigma_g)^{-1}$ $(1\pi_u)^{-2}$ $(1\pi_g)^2$
			0.17 $(3\sigma_g)^{-1}$ $(1\pi_u)^{-2}$ $(n\pi_u)^2$
			0.08 $(2\sigma_g)^{-1}$
	31.15	0.016	0.61 $(2\sigma_u)^{-1}$ $(1\pi_u)^{-1}$ $(n\pi_g)^1$
			0.55 $(3\sigma_g)^{-1}$ $(1\pi_u)^{-2}$ $(1\pi_g)^2$
			0.26 $(3\sigma_g)^{-1}$ $(1\pi_u)^{-1}$ $(n\pi_u)^1$
			0.13 $(1\pi_u)^{-2}$ $(n\delta_g)^1$
			0.11 $(2\sigma_g)^{-1}$ $(1\pi_u)^{-2}$ $(1\pi_g)^2$
			0.09 $(2\sigma_g)^{-1}$
			0.07 $(3\sigma_g)^{-1}$
	31.66	0.016	0.78 $(3\sigma_g)^{-1}$ $(1\pi_u)^{-1}$ $(n\pi_u)^1$
			0.26 $(2\sigma_u)^{-1}$ $(1\pi_u)^{-1}$ $(n\pi_g)^1$
			0.25 $(3\sigma_g)^{-1}$ $(1\pi_u)^{-2}$ $(n\pi_u)^2$
			0.20 $(2\sigma_u)^{-1}$ $(1\pi_u)^{-2}$ $(n\pi_g)^1$ $(n\pi_u)^1$
			0.13 $(3\sigma_g)^{-1}$ $(2\sigma_u)^{-1}$ $(n\sigma_u)^1$
			0.13 $(3\sigma_g)^{-1}$
	32.23	0.004	0.93 $(3\sigma_g)^{-1}$ $(1\pi_u)^{-2}$ $(1\pi_g)^2$
	34.26	0.005	0.87 $(1\pi_u)^{-2}$ $(n\delta_g)^1$
			0.18 $(3\sigma_g)^{-1}$ $(1\pi_u)^{-2}$ $(1\pi_g)^2$)
$^2\Pi_g$	23.74[f]	0.026	0.90 $(1\pi_u)^{-2}$ $(1\pi_g)^1$
$^2\Pi_u$	11.40	1.64	0.93 $(1\pi_u)^{-1}$
			0.14 $(1\pi_u)^{-2}$ $(n\pi_u)^1$
	26.86	0.015	0.88 $(1\pi_u)^{-2}$ $(n\pi_u)^1$
			0.10 $(1\pi_u)^{-1}$
	31.65	0.005	0.62 $(1\pi_u)^{-1}$ $(3\sigma_g)^{-1}$ $(n\sigma_g)^1$
			0.44 $(1\pi_u)^{-2}$ $(n\pi_u)^1$

Downloaded¬11¬Dec¬2003¬to¬137.82.31.98. Redistribution¬subject¬to¬AIP¬license¬or¬copyright,¬see¬http://ojps.aip.org/jcpo/jcpcr.jsp

TABLE IV. (*Continued*.)

Symmetry	Ionization energy (eV)[d]	Intensity[b] (S_j^2)	Important configurations[c]
			0.31 $(1\pi_u)^{-1}$ $(2\sigma_u)^{-1}$ $(n\sigma_u)^1$
	32.03	0.011	0.64 $(1\pi_u)^{-1}$ $(2\sigma_u)^{-1}$ $(n\sigma_u)^1$
			0.35 $(1\pi_u)^{-2}$ $(n\pi_u)^1$
			0.32 $(1\pi_u)^{-1}$ $(3\sigma_g)^{-1}$ $(n\sigma_g)^1$
			0.31 $(3\sigma_g)^{-1}$ $(2\sigma_u)^{-1}$ $(1\pi_g)^1$
			0.07 $(1\pi_u)^{-1}$
	36.08	0.010	0.53 $(1\pi_u)^{-2}$ $(n\pi_u)^1$
			0.47 $(1\pi_u)^{-1}$ $(3\sigma_g)^{-1}$ $(n\sigma_g)^1$
			0.44 $(1\pi_u)^{-1}$ $(2\sigma_u)^{-1}$ $(n\sigma_u)^1$
$^2\Sigma_u^+$	18.69	0.705	0.87 $(2\sigma_u)^{-1}$
			0.27 $(3\sigma_g)^{-1}$ $(1\pi_u)^{-1}$ $(1\pi_g)^1$
			0.14 $(2\sigma_u)^{-1}$ $(1\pi_u)^{-1}$ $(n\pi_u)^1$
			0.13 $(2\sigma_g)^{-1}$ $(1\pi_u)^{-1}$ $(1\pi_g)^1$
	23.82	0.010	0.89 $(3\sigma_g)^{-1}$ $(1\pi_u)^{-1}$ $(1\pi_g)^1$
			0.19 $(1\pi_u)^{-2}$ $(n\sigma_u)^1$
			0.14 $(2\sigma_u)^{-1}$ $(1\pi_u)^{-2}$ $(1\pi_g)^2$
			0.10 $(2\sigma_u)^{-1}$
	25.13	0.018	0.88 $(1\pi_u)^{-2}$ $(n\sigma_u)^1$
			0.17 $(3\sigma_g)^{-1}$ $(1\pi_u)^{-1}$ $(1\pi_g)^1$
			0.13 $(2\sigma_u)^{-1}$
	30.31	0.029	0.82 $(3\sigma_g)^{-1}$ $(1\pi_u)^{-1}$ $(n\pi_g)^1$
			0.24 $(2\sigma_u)^{-1}$ $(1\pi_u)^{-2}$ $(1\pi_g)^2$
			0.14 $(2\sigma_u)^{-1}$
	32.79	0.004	0.68 $(2\sigma_u)^{-1}$ $(1\pi_u)^{-1}$ $(n\pi_u)^1$
			0.47 $(3\sigma_g)^{-1}$ $(1\pi_u)^{-1}$ $(n\pi_g)^1$
			0.24 $(2\sigma_g)^{-1}$ $(1\pi_u)^{-1}$ $(n\pi_g)^1$
			0.17 $(2\sigma_u)^{-1}$ $(1\pi_u)^{-2}$ $(1\pi_g)^2$
			0.09 $(2\sigma_u)^{-1}$
	34.07	0.004	0.73 $(1\pi_u)^{-3}$ $(n\pi_g)^1$ $(n\sigma_g)^1$
			0.33 $(2\sigma_u)^{-1}$ $(1\pi_u)^{-1}$ $(n\pi_u)^1$
			0.30 $(3\sigma_g)^{-1}$ $(1\pi_u)^{-1}$ $(n\pi_g)^1$
			0.21 $(2\sigma_u)^{-1}$ $(1\pi_u)^{-2}$ $(1\pi_g)^2$
			0.09 $(2\sigma_u)^{-1}$
	34.12	0.013	0.54 $(3\sigma_g)^{-1}$ $(1\pi_u)^{-1}$ $(n\pi_g)^1$
			0.44 $(2\sigma_u)^{-1}$ $(1\pi_u)^{-1}$ $(n\pi_u)^1$
			0.40 $(1\pi_u)^{-3}$ $(n\pi_g)^1$ $(n\sigma_g)^1$
			0.09 $(2\sigma_u)^{-1}$

[a]For each symmetry, the MRSDCI wave functions are used for the cation and neutral molecule, and all calculations are based on the frozen average natural orbitals.

[b]The values less than 0.004 are ignored. All π_u and π_g intensities have been multiplied by two.

[c]Absolute value is used for every Cl coefficient.

[d]The first root energies have been adjusted to experimental data separately for each symmetry except for the $^2\Pi_g$ symmetry, and the same constant shift is used for the remaining roots in this symmetry. For symmetry $^2\Sigma_g^+$, the energy shift is -0.66 eV (to the lower binding energy direction), for symmetry $^2\Pi_u$ -0.12 eV and for symmetry, $^2\Sigma_u^+$ -0.45 eV.

[f]The energy of the ground state of the neutral molecule is taken from our MRSDCI calculation based on the ionic frozen average natural orbitals of this symmetry ($^2\Pi_g$).

nal EMS experimental momentum profiles measured in the binding energy range of satellite 4 [see Fig. 6(c) of Ref. 19 and Fig. 7(b) of Ref. 20] shows a broader momentum profile than the predicted momentum distribution if the peak was associated only with the $2\sigma_g^{-1}$ process. A more likely explanation for the broad experimental momentum profile (extra intensity in the region $p=1-2$ a.u.) measured by Weigold *et al.* would be to assign peak 4 mainly with the $3\sigma_g^{-1}$ process. It is well known that the $3\sigma_g$ momentum distribution is wider (i.e., contains significant high momentum components) than the $2\sigma_g$ momentum distribution[19,20] and thus the $3\sigma_g$ wave function would fit the original EMS data better.

Weigold *et al.* argued that the extra intensity at high momentum observed in the satellite 4 experimental momentum profile is due to well known distortion effects (i.e., breakdown of the plane wave impulse approximation) and therefore satellite 4 is associated with the $2\sigma_g^{-1}$ process. This argument seems inconsistent since distortion effects are not seen in the experimental momentum profiles of the main $2\sigma_g^{-1}$ peak obtained in the same experiment. The present MRSDCI calculations and synchrotron PES observations regarding the sat.$4/2\sigma_g$ main peak intensity ratios (see above) indicate that a more consistent explanation would be to regard peak 4 as associated with the $3\sigma_g^{-1}$ process instead. A high energy resolution EMS study of satellite 4 in acetylene (with very good statistics) will provide further information to decide which of the alternative explanations presented is more likely.

Downloaded¬11¬Dec¬2003¬to¬137.82.31.98. Redistribution¬subject¬to¬AIP¬license¬or¬copyright,¬see¬http://ojps.aip.org/jcpo/jcpcr.jsp

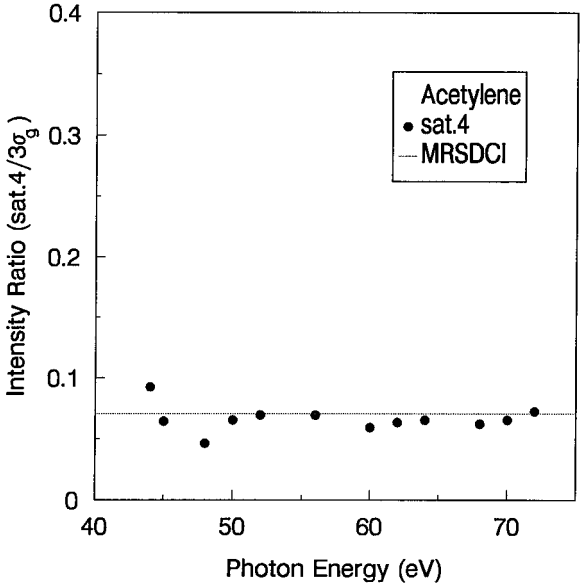

FIG. 5. Normal acetylene and Isotopically labeled acetylene: photon energy dependence of the intensity ratio of satellite 4 (31.2 eV binding energy). The intensity ratios are taken relative to the $3\sigma_g^{-1}$ main peak at binding energy of 16.36 eV. All reported intensity ratios are corrected for transmission effects. The MRSDCI value was obtained by summing all the pole strengths in 31–33 eV and dividing by the pole strengths in 16–17 eV (see Table IV).

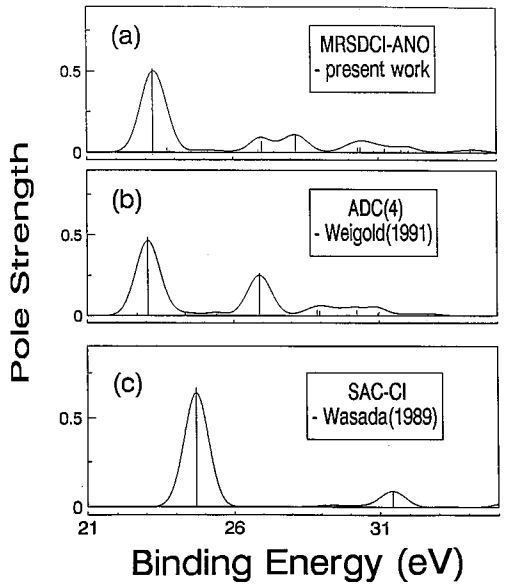

FIG. 6. Comparison of the calculated photoelectron spectra obtained in the present work (a) with those reported by Weigold *et al.* (Ref. 19) (b), and Wasada and Hirao (Ref. 17) (c). The SAC-CI calculation predicts pole strengths at binding energies >35 eV which are not included in the present diagram. The calculated pole strengths (solid poles) are convoluted with the experimental peak widths to yield the solid curve which can then be compared with experiment.

The experimental PES spectrum and the theoretical PES spectrum obtained from MRSDCI calculations are compared in Fig. 4. As can be seen there is reasonable agreement between experiment and theory in the inner valence region. This is the first PES study on acetylene that includes both theoretical and experimental results with semiquantitative agreement. The theoretical results lend support to the assignment of largely $^2\Sigma_g^+$ symmetry for the satellites 1–4. It can be seen from Fig. 4(b) that most of the dominant poles are associated with the $2\sigma_g^{-1}$ and $3\sigma_g^{-1}$ ionization processes and are indicated by (*). Furthermore, these theoretical results show that there are contributions to the intensity of satellites 1, 3, and 4 from $1\pi_u^{-1}$, $3\sigma_g^{-1}$, and $2\sigma_u^{-1}$ as well as $2\sigma_g^{-1}$ ionization process, i.e., there is inter-leaving of correlation states. It is likely that the intensity ratio variations of correlation peaks 1, 3, and 4 are due to intensity contributions from more than one symmetry. Before proceeding with the discussion of the correlation peaks 1–4, we should note that the MRSDCI calculations predict some correlation states within the main $2\sigma_g^{-1}$ envelope itself. A $^2\Pi_g$ correlation state is predicted at 23.74 eV and a $^2\Sigma_u$ correlation state is predicted at 23.82 eV. These theoretical results are also consistent with experiment (Fig. 1) which showed an unusually broad $2\sigma_g^{-1}$ main peak which is represented by three Gaussian peaks in the deconvolution. The exact location of the correlation peak corresponding to the $^2\Pi_g$ state can not be quoted with certainty because there is no clear shoulder in the experimental data. The $^2\Pi_g$ state predicted at 23.74 eV is of special interest because it is largely due to initial state configuration interaction (i.e., the $1\pi_g$ orbital is unoccupied in the Hartree–Fock neutral configuration).

According to the MRSDCI calculations (see Table IV), satellite 2 can be considered as purely of $^2\Sigma_g^+$ symmetry ($2\sigma_g^{-1}$) and its intensity ratio relative to the $2\sigma_g^{-1}$ main peak (see Figs. 2 and 3), in fact, shows the least variation from the predicted constant trend expected for an intrinsic correlation state. The MRSDCI calculations indicate a single correlation state at 28.13 eV associated mainly with a $2h-1p$ configuration, $(1\pi_u)^{-2}(n\delta_g)^1$. There are no correlation states of other symmetry which is of significant intensity in the binding energy region of satellite 2. Satellites 1 and 4 are dominated by correlation states of $^2\Sigma_g^+$ symmetry ($2\sigma_g^{-1}$ and $3\sigma_g^{-1}$) with some contributions from $^2\Pi_u$ and $^2\Sigma_u^+$ correlation states. Satellite 3 is still largely of $^2\Sigma_g^+$ symmetry but contains a $^2\Sigma_u^+$ correlation state of large pole strength. The cummulative pole strength of $^2\Sigma_g^+$ correlation states in the 30–31 eV binding energy range is 0.054 while the single $^2\Sigma_u^+$ correlation state at 30.31 eV has a comparable pole strength of 0.029. Thus the observed variations in the intensity ratios for satellite 3 are clearly consistent with the theoretical predictions which indicate several correlation states of different symmetry. The MRSDCI calculations also show an extra peak at 34 eV binding energy. This corresponds to peak 5 observed by Svensson *et al.*[12] and is beyond the energy range of the present synchrotron PES study. The present MRSDCI calculations predict that peak 5 is of $^2\Sigma_u$ symmetry (see Table IV). Another point that should be mentioned is the relative importance of 3-hole-2-particle ($3h-2p$) ionic configurations in $C_2H_2^+$ compared to $C_2H_4^+$.[28] This is related to the relative ease of forming three holes in acetylene (which has four π-electrons) than in ethylene (which has two π-electrons).

We now compare the present MRSDCI (ANO) calculations with other recently published theoretical calculations in Fig. 6. In general, other theoretical calculations (Fig. 6) do

Downloaded¬11¬Dec¬2003¬to¬137.82.31.98. Redistribution subject to AIP license or copyright,¬see¬http://ojps.aip.org/jcpo/jcpcr.jsp

not show as good an agreement as our MRSDCI results with the experimental results (Fig. 1). The previously reported calculations seem to suffer from limitations in their basis sets. For example, Weigold *et al.*[19] use a 58-CGTOs basis set in their ADC(4) Green's function calculations, and Wasada and Hirao[20] use a 42-CGTOs basis set in their SAC (CI) calculations. The 58-CGTO and 42-CGTO basis sets do not include sufficient basis functions to represent excited states of the ion. For example, the 58-CGTO basis set of Weigold *et al.* has only one set of *d*-type polarization function on each carbon atom thus can form only one set of δ_g basis functions. In comparison, the present MRSDCI basis set is capable of forming seven sets of δ_g basis functions. Previous theoretical calculations prior to 1989 are not included in the comparison. An extended $2p-1h$ TDA Green's function [equivalent to ADC(3)] calculation on acetylene has been presented in graphical form [Fig. 5(c) in Ref. 3] but not in tabular form. The results of this particular calculation is similar in some respects to the ADC(4) calculation of Weigold *et al.* It should be noted that the older version $2h-1p$ TDA Green's function calculation is a ''cheap and quick calculation and not expected to be quantitative.''[48] More recent versions of the Green's function method such as ADC(3) and ADC(4) are believed to be more quantitative if appropriate basis sets are employed.

The present MRSDCI (ANO) study uses a 171-CGTOs basis set which includes several Rydberg orbitals and diffuse functions. The improvement in the results can be observed by comparing each theoretical calculation with the experimental PES spectrum (cf. Figs. 4 and 6). The MRSDCI(ANO) calculations are, clearly, superior in terms of the prediction of the binding energies and peak intensities (see Figs. 2 and 4). The SAC-CI calculation of Wasada and Hirao [Fig. 5(c)] is unsatisfactory in an overall sense. In particular, the SAC-CI calculation predicts two $^2\Sigma_u^+$ correlation states in the 26–32 eV region which is not consistent with the present experimental and theoretical results. The SAC-CI calculation predicts the first correlation state at $\approx$31 eV whereas experiment clearly shows the correlation peak at much lower binding energy (25.56 eV). The symmetry assignments of the SAC-CI calculation is also inconsistent with EMS measurements[19,20] and ADC(4) calculations.[19]

The ADC(4) calculation of Weigold *et al.* is a significant improvement compared to the SAC-CI calculation. The overall profile of the ADC(4) calculation agrees better with the present experimental results except that it predicts only one main correlation state in the binding energy region of correlation peaks 1 and 2. These twin peaks (1 and 2) are clearly resolved in the present experiment as well as previous XPS measurements. The shortcoming of the most advanced Green's function calculation [ADC(4)] for acetylene may be due to the basis set chosen as opposed to the method itself. It has been observed in the MRSDCI calculation of the photoelectron spectrum of ethylene that ''twining effects'' are very sensitive to the choice of basis set.[27,28]

V. SUMMARY

The present study show a high level of agreement obtained between high-resolution synchrotron photoelectron spectra of acetylene and the predicted inner valence binding energy spectra using a recent MRSDCI(ANO) pole strength calculation. The present experimental PES results, taken at 40–75 eV photon energy, are also consistent with the previous XPS[15] and EMS[19,20] measurements with regards to the energy position and the symmetry assignment of the inner valence and correlation peaks of acetylene. Slight differences in the observed correlation peak intensity ratios can be explained on the basis of variation in the C_{2p}/C_{2s} atomic photoionization cross section as a function of photon energy. The symmetry assignments (mainly $^2\Sigma_g$) of correlation peaks 1, 2, 3, and 4 of acetylene obtained from the present study (experimental and theory) are in general agreement with electron momentum spectroscopy experiments.[19,20] The photon energy dependence of the correlation peak intensities (1, 2, 3, and 4) relative to the $2\sigma_g$ main peak indicate that peaks 1, 2, and 3 are ''intrinsic'' correlation peaks associated with the $2\sigma_g^{-1}$ ionization process. In contrast, correlation peak 4 may be considered an intrinsic correlation peak associated mainly with the $3\sigma_g^{-1}$ ionization process as opposed to the $2\sigma_g^{-1}$ ionization process or may be a dynamic correlation peak associated with the $2\sigma_g^{-1}$ ionization process. It is important to experimentally resolve whether peak 4 is associated mainly with the $2\sigma_g^{-1}$ or with the $3\sigma_g^{-1}$ process. A high energy resolution EMS study of good statistics on peak 4 may be useful. Future work also may include intensity ratio measurements at higher energies (>80 eV), particularly for satellite 2 which shows constant intensity ratio in range of about 40–72 eV photon energy, yet seems to increase in intensity at x-ray energies.

ACKNOWLEDGMENTS

We would like to acknowledge the assistance of the staff of the Synchrotron Radiation Center, University of Wisconsin. This work was funded by the Natural Sciences and Engineering Research Council of Canada. Work at Indiana University was supported by the National Science Foundation.

[1] S. Wilson, *Electron Correlation in Molecules* (Oxford University, Oxford, 1984).
[2] G. Bieri and L. Åsbrink, J. Electron Spectrosc. **20**, 149 (1980).
[3] L. S. Cederbaum, W. Domcke, J. Schrimer, and W. von Niessen, Adv. Chem. Phys. **65**, 115 (1986).
[4] C. L. French, C. E. Brion, and E. R. Davidson, Chem. Phys. **122**, 247 (1988).
[5] S. Krummacher, V. Schmidt, and F. Wuilleumier, J. Phys. B **13**, 3993 (1980).
[6] S. Krummacher, V. Schmidt, F. Wuillemuier, J. M. Bizau, and D. Ederer, J. Phys. B **16**, 1733 (1983).
[7] U. Becker and D. A. Shirley, Phys. Scr. T **31**, 51 (1990).
[8] A. J. Dixon, I. E. McCarthy, E. Weigold, and G. R. J. Williams, J. Electron Spectrosc. **12**, 239 (1977).
[9] R. G. Cavell and D. A. Allison, J. Chem. Phys. **69**, 159 (1978).
[10] A. M. Bradshaw, W. Eberhardt, H. J. Levinson, W. Domcke, and L. S. Cederbaum, Chem. Phys. Lett. **70**, 36 (1980).
[11] J. Müller, R. Arneberg, H. Ågren, R. Manne, P.-Å. Malmquist, S. Svensson, and U. Gelius, J. Chem. Phys. **77**, 4895 (1982).
[12] S. Svensson, P.-Å. Malmquist, M. Y. Adam, P. Lablanquie, P. Morin, and I. Nenner, Chem. Phys. Lett. **111**, 574 (1984).
[13] L. S. Cederbaum, W. Domcke, J. Schirmer, W. Von Niessen, G. H. F. Diercksen, and W. P. Kraemer, J. Chem. Phys. **69**, 1591 (1978).
[14] A. M. Bradshaw, W. Eberhardt, H. J. Levinson, W. Domcke, and L. S. Cederbaum, Chem. Phys. Lett. **70**, 36 (1980).

Downloaded¬11¬Dec¬2003¬to¬137.82.31.98. Redistribution¬subject¬to¬AIP¬license¬or¬copyright,¬see¬http://ojps.aip.org/jcpo/jcpcr.jsp

[15] S. Svensson, E. Zdansky, U. Gelius, and H. Ågren, Phys. Rev. A **37**, 4730 (1988).
[16] Delano P. Chong, Can. J. Chem. **63**, 2007 (1985).
[17] H. Wasada and K. Hirao, Chem. Phys. **138**, 227 (1989).
[18] A. Koch, M. Schmidbauer, J. Feldhaus, K. J. Randall, and A. M. Bradshaw, J. Electron. Spectrosc. **51**, 527 (1990).
[19] E. Weigold, K. Zhao, and W. Von Niessen, J. Chem. Phys. **94**, 3468 (1991).
[20] Patrick Duffy, S. A. C. Clark, C. E. Brion, Mark E. Casida, D. P. Chong, E. R. Davidson, and C. Maxwell, Chem. Phys. **165**, 183 (1992).
[21] R. Arneberg, H. Ågren, R. Manne, P.-Å. Malmquist, and S. Svensson, Chem. Phys. Lett. **92**, 125 (1982).
[22] P. R. Keller, D. Mehaffy, J. W. Taylor, F. A. Grimm, and T. A. Carlson, J. Electron Spectrosc. **27**, 223 (1982).
[23] Z. H. Levine and P. Soven, Phys. Rev. Lett. **50**, 2074 (1983).
[24] A. C. Parr, D. L. Ederer, J. B. West, D. M. P. Holland, and J. L. Dehemer, J. Chem. Phys. **76**, 4349 (1982).
[25] J. D. Bozek, J. N. Cutler, G. M. Bancroft, L. L. Coatsworth, K. H. Tan, D. S. Yang, and R. G. Cavell, Chem. Phys. Lett. **165**, 1 (1990).
[26] A. D. O. Bawagan, B. J. Olsson, K. H. Tan, J. M. Chen, and B. X. Yang, Chem. Phys. **164**, 283 (1992).
[27] S. J. Desjardins, A. D. O. Bawagan, K. H. Tan, Y. Wang, and E. R. Davidson, Chem. Phys. Lett. **227**, 519 (1994).
[28] S. J. Desjardins, A. D. O. Bawagan, Z. F. Liu, K. H. Tan, Y. Wang, and E. R. Davidson, J. Chem. Phys. **102**, 6385 (1995).
[29] J. Schirmer, M. Braunstein, and V. McCoy, Phys. Rev. A **44**, 5762 (1991).
[30] G. Bandarage and R. R. Lucchese, Phys. Rev. A **47**, 1989 (1993).
[31] H. Partridge, *Near Hartree–Fock Quality GTO Basis Sets for the Second-Row Atoms*, NASA Technical Memorandum 89449, 73 (1987).
[32] H. Partridge, *Near Hartree–Fock Quality GTO Basis Sets for the First- and Third-Row Atoms*, NASA Technical Memorandum 101044, 73 (1989).
[33] C. J. Maxwell, F. B. C. Machado, and E. R. Davidson, J. Am. Chem. Soc. **114**, 6496 (1992).
[34] W. Dunning, Jr., J. Chem. Phys. **90**, 1007 (1989).
[35] W. J. Hunt and W. A. Goddard III, Chem. Phys. Lett. **3**, 414 (1969).
[36] Y. Wang, Ph.D. thesis, Indiana University, 1994.
[37] K. Kimura, S. Katsuwata, Y. Achiba, T. Yamazaki, and S. Iwata, *Handbook of Hel Photoelectron Spectra of Fundamental Organic Molecules* (Halsted, New York, 1981).
[38] M. Sabaye-Moghaddam, MSc. thesis, Carleton University, 1995.
[39] A. A. Wills, A. A. Cafolla, A. Svensson, and J. Comer, J. Phys. B **23**, 2013 (1990).
[40] J. A. R. Samson, Y. Chung, and E. M. Lee, Phys. Rev. A **45**, 259 (1992).
[41] J. J. Yeh and I. Lindau, At. Data Nucl. Data Tables **32**, 1 (1985).
[42] T. Ishihara, J. Mizuno, and T. Watanabe, Phys. Rev. A **22**, 1552 (1980).
[43] J. A. R. Samson, Phys. Rev. Lett. **22**, 693 (1969).
[44] F. Wuilleumier, M. Y. Adam, N. Sandner, and V. Schmidt, J. Phys. (Paris) Lett. **41**, L373 (1980).
[45] T. A. Ferrett, D. W. Lindle, P. A. Heimann, W. D. Brewer, U. Becker, H. G. Kerkhoff, and D. A. Shirley, Phys. Rev. A **36**, 3172 (1987).
[46] U. Becker *et al.* (1989), quoted on p. 1591 in V. Schmidt, Rep. Prog. Phys. **55**, 1483 (1992).
[47] T. Reich, P. A. Heimann, B. L. Petersen, E. Hudson, Z. Hussain, and D. A. Shirley, Phys. Rev. A **49**, 4570 (1994).
[48] L. S. Cederbaum (private communication).

Downloaded¬11¬Dec¬2003¬to¬137.82.31.98. Redistribution¬subject¬to¬AIP¬license¬or¬copyright,¬see¬http://ojps.aip.org/jcpo/jcpcr.jsp